



## **Osteoclastic and Osteoblastic Responses to Hypergravity and Microgravity: Analysis Using Goldfish Scales as a Bone Model**

Authors: Yamamoto, Tatsuki, Ikegame, Mika, Furusawa, Yukihiro, Tabuchi, Yoshiaki, Hatano, Kaito, et al.

Source: Zoological Science, 39(4) : 388-396

Published By: Zoological Society of Japan

URL: <https://doi.org/10.2108/zs210107>

---

BioOne Complete ([complete.BioOne.org](https://complete.BioOne.org)) is a full-text database of 200 subscribed and open-access titles in the biological, ecological, and environmental sciences published by nonprofit societies, associations, museums, institutions, and presses.

Your use of this PDF, the BioOne Complete website, and all posted and associated content indicates your acceptance of BioOne's Terms of Use, available at [www.bioone.org/terms-of-use](https://www.bioone.org/terms-of-use).

Usage of BioOne Complete content is strictly limited to personal, educational, and non - commercial use. Commercial inquiries or rights and permissions requests should be directed to the individual publisher as copyright holder.

---

BioOne sees sustainable scholarly publishing as an inherently collaborative enterprise connecting authors, nonprofit publishers, academic institutions, research libraries, and research funders in the common goal of maximizing access to critical research.

# Osteoclastic and Osteoblastic Responses to Hypergravity and Microgravity: Analysis Using Goldfish Scales as a Bone Model

Tatsuki Yamamoto<sup>1</sup>, Mika Ikegame<sup>2</sup>, Yukihiro Furusawa<sup>3</sup>, Yoshiaki Tabuchi<sup>4</sup>, Kaito Hatano<sup>1</sup>, Kazuki Watanabe<sup>5</sup>, Umi Kawago<sup>1</sup>, Jun Hirayama<sup>6</sup>, Sachiko Yano<sup>7</sup>, Toshio Sekiguchi<sup>1</sup>, Kei-ichiro Kitamura<sup>8</sup>, Masato Endo<sup>9</sup>, Arata Nagami<sup>10</sup>, Hajime Matsubara<sup>10</sup>, Yusuke Maruyama<sup>5</sup>, Atsuhiko Hattori<sup>5</sup>, and Nobuo Suzuki<sup>1\*</sup>

<sup>1</sup>*Noto Marine Laboratory, Institute of Nature and Environmental Technology, Kanazawa University, Housu-gun, Ishikawa 927-0553, Japan*

<sup>2</sup>*Department of Oral Morphology, Okayama University Graduate School of Medicine, Dentistry and Pharmaceutical Sciences, Okayama, Okayama 700-8525, Japan*

<sup>3</sup>*Department of Pharmaceutical Engineering, Faculty of Engineering, Toyama Prefectural University, Kurokawa, Toyama 939-0398, Japan*

<sup>4</sup>*Life Science Research Center, University of Toyama, Sugitani, Toyama 930-0194, Japan*

<sup>5</sup>*Department of Biology, College of Liberal Arts and Sciences, Tokyo Medical and Dental University, Ichikawa, Chiba 272-0827, Japan*

<sup>6</sup>*Department of Clinical Engineering, Faculty of Health Sciences, Komatsu University, Komatsu, Ishikawa 923-0961, Japan*

<sup>7</sup>*Japan Aerospace Exploration Agency, Tsukuba, Ibaraki 305-8505, Japan*

<sup>8</sup>*Department of Clinical Laboratory Science, Division of Health Sciences, Graduate School of Medical Science, Kanazawa University, Kodatsuno, Ishikawa 920-0942, Japan*

<sup>9</sup>*Laboratory of Fish Culture, Tokyo University of Marine Science and Technology, Minato-ku, Tokyo 108-8477, Japan*

<sup>10</sup>*Noto Center for Fisheries Science and Technology, Kanazawa University, Ossaka, Noto-cho, Ishikawa 927-0552, Japan*

It is known that the bone matrix plays an important role in the response to physical stresses such as hypergravity and microgravity. In order to accurately analyze the response of bone to hypergravity and microgravity, a culture system under the conditions of coexistence of osteoclasts, osteoblasts, and bone matrix was earnestly desired. The teleost scale is a unique calcified organ in which osteoclasts, osteoblasts, and the two layers of bone matrix, i.e., a bony layer and a fibrillary layer, coexist. Therefore, we have developed in vitro organ culture systems of osteoclasts and osteoblasts with the intact bone matrix using goldfish scales. Using the scale culture system, we examined the effects of hypergravity with a centrifuge and simulated ground microgravity (g- $\mu$ G) with a three-dimensional clinostat on osteoclasts and osteoblasts. Under 3-gravity (3G) loading for 1 day, osteoclastic marker mRNA expression levels decreased, while the mRNA expression of the osteoblastic marker increased. Upon 1 day of exposure, the simulated g- $\mu$ G induced remarkable enhancement of osteoclastic marker mRNA expression, whereas the osteoblastic marker mRNA expression decreased. In response to these gravitational stimuli, osteoclasts underwent major morphological changes. By simulated g- $\mu$ G treatments, morphological osteoclastic activation was induced, while osteoclastic deactivation was observed in the 3G-treated scales. In space experiments, the results that had been obtained with simulated g- $\mu$ G were reproduced. RNA-sequencing analysis showed that osteoclastic activation was induced by the down-regulation of Wnt signaling under flight-microgravity. Thus, goldfish scales can be utilized as a bone model to analyze the responses of osteoclasts and osteoblasts to gravity.

**Key words:** hypergravity, microgravity, osteoclasts, osteoblasts, fish scales, bone metabolism, goldfish, biological space experiments

## INTRODUCTION

Bone is an active connective tissue that is composed of

three types of cells: osteoclasts, osteoblasts, and osteocytes (Civitelli, 2008; Schaffler and Kennedy, 2012; Chen et al., 2018). Osteoclasts are bone-resorptive cells that elute bone matrixes by several enzymes, while osteoblasts are bone-formative cells that secrete bone matrix to form hard bone. The physical stimuli function in these bone cells

\* Corresponding author. E-mail: nobuos@staff.kanazawa-u.ac.jp  
doi:10.2108/zs210107

directly or indirectly and play an essential role in the regulation of bone remodeling (Carmeliet et al., 2001; Civitelli, 2008). However, the process of translating the physical stimulus into a biological response, called *mechanotransduction*, is poorly understood now due to the lack of a suitable in vitro model system. Furthermore, in the response to physical stimuli, the bone matrix plays an important role (Harter et al., 1995; Owan et al., 1997; Hoffer et al., 2006). Watabe et al. (2011) reported that the  $\alpha_5\beta_1$  integrin, which participates in cell adhesion with the bone matrix, plays an important role in mechanotransduction. In order to accurately analyze the bone metabolism response to physical stimuli such as hypergravity and microgravity, therefore, an in vitro culture system under the conditions of coexistence with osteoclasts, osteoblasts, and bone matrix was earnestly desired.

On the other hand, the teleost scale is a unique calcified tissue in which osteoclasts, osteoblasts, and the two layers of the bone matrix, i.e., a bony layer, which is a thin, well-calcified external layer, and a fibrillary layer, which is a thick, partially calcified layer, coexist (Bereiter-Hahn and Zylberberg, 1993; Ohira et al., 2007; Suzuki et al., 2007; Ikegame et al., 2019). The bone matrix, which includes type I collagen (Zylberberg et al., 1992), osteocalcin (Nishimoto et al., 1992), and hydroxyapatite (Onozato et al., 1979), is present in scale as well as in mammalian bone. Furthermore, we recently demonstrated that osteocyte-like cells exist in goldfish scales (Yamamoto et al., 2020a). Since osteocytes are known to be the principal sensors for the mechanical loading of bone in mammals (Tatsumi et al., 2007; Lin et al., 2009; Schaffler and Kennedy, 2012; Alford et al., 2015; Smith, 2020), it is possible to use fish scales to study the response to physical stimuli.

In the present study, the scale organ culture system developed previously (Suzuki et al., 2000; Suzuki and Hattori, 2002; Omori et al., 2012) was used to examine the effects of hypergravity with a centrifuge and simulated ground microgravity (g- $\mu$ G) with a three-dimensional (3D) clinostat on osteoclasts and osteoblasts. To confirm the results obtained with simulated microgravity, we performed experiments in space and examined the influence of flight-microgravity (f- $\mu$ G) on bone metabolism. We are the first to indicate hypergravity and microgravity impacts on osteoclasts morphologically, and we demonstrated that the Wnt signal pathway plays an important role in the response of both osteoclasts and osteoblasts to hypergravity and microgravity.

## MATERIALS AND METHODS

### Animals

Goldfish (*Carassius auratus*) were purchased from a commercial source (Higashikawa Fish Farm, Yamatokoriyama, Japan) and artificially fertilized from one pair of female and male goldfish (20–30 g) in the Laboratory of Fish Culture, Tokyo University of Marine Science and Technology. The hatched fish were fed brine shrimp for bait and then were given a commercial formula feed. Thereafter, the fish were fed a commercial pellet diet for sea bream every morning and were maintained in fresh water at 26°C. Growing fish (body length: 12–15 cm) were transferred to Noto Marine Laboratory of Kanazawa University and Tokyo Medical and Dental University and used for in vitro experiments analyzing mRNA expression and morphological studies.

All experimental procedures were conducted in accordance

with the Guide for the Care and Use of Laboratory Animals prepared by Kanazawa University and Tokyo Medical and Dental University.

### Preparation of regenerating scales in goldfish

Teleost scale regenerates after being removed. We previously reported that the osteogenesis in regenerating scales was very similar to that in calvarial bone (mammalian head bone) (Yoshikubo et al., 2005). Osteoblastic activity in the regenerating scale was considerably higher than that in normal scale (Yoshikubo et al., 2005; Suzuki et al., 2009; Thamamongood et al., 2012). Therefore, we used regenerating scales and examined the influence of hypergravity and simulated microgravity (g- $\mu$ G) on osteoclasts and osteoblasts.

Full-grown scales were removed from the goldfish, which had been anesthetized with 0.03% ethyl 3-aminobenzoate methanesulfonic acid salt (Sigma-Aldrich, Inc., St. Louis, MO, USA), to allow for the regeneration of scales. Their scales were removed one by one in two horizontal, bilateral lines using sharpened forceps. Subsequently, the goldfish were kept with a 12-h:12-h light–dark cycle (light turned on at 8:00 a.m.) at 26°C. On day 12 after the removal of their scales, the goldfish were bred in water with the anti-infection reagent F Gold (Japan Pet Design Co., Ltd., Tokyo, Japan). Subsequently, regenerating scales were sampled on day 14 from goldfish on ice that had been sterilized using hypochlorous and fungicide solutions and immersed in Leibovitz's L-15 medium (Invitrogen, Grand Island, NY, USA) containing 10% FCS (Nichirei Biosciences, Inc., Tokyo, Japan), 100 U/mL penicillin, 100  $\mu$ g/mL streptomycin, and 200  $\mu$ g/mL kanamycin.

### Hypergravity and simulated g- $\mu$ G treatments of regenerating scales in goldfish

Sterilized scales were put into 96-well plates (one scale per well). The lines of the left side were used as an experimental group, while the lines of the opposite side were adopted as a control group. In the loading, different parallel experiments using 10 goldfish were conducted. The 96-well plates containing the scales were loaded to 3-gravity (3G) using a centrifuge (LIX-130, Tomy Digital Biology Co., Ltd., Tokyo, Japan) for 1 day (Suzuki et al., 2008). After centrifugation was finished, the incubated scales were put into RNAlater (Sigma-Aldrich, St. Louis, MO, USA) and then frozen at –80°C for mRNA analysis.

In the case of simulated g- $\mu$ G with 3D clinostat treatments, the regenerating scales were prepared as described above and put into 96-well plates (one scale per well). In the present study, different parallel experiments using 10 goldfish were conducted. Plates containing scales were treated to simulate g- $\mu$ G using a 3D clinostat (Toray Engineering Co., Ltd., Tokyo, Japan) (Figure S1) for one day. After unloading by a 3D clinostat, the scales were stocked in RNAlater (Sigma-Aldrich) at –80°C until mRNA expression analysis.

### Changes in osteoclastic and osteoblastic marker mRNA expression in hypergravity- and simulated g- $\mu$ G-treated scales

We examined changes in osteoclastic (*cathepsin K: Ctsk*; *tartrate-resistant acid phosphatase: Trap*; *osteoclast stimulatory transmembrane protein: Oc-stamp*; *integrin beta-3: Itgb3*; *cellular Src: c-Src*) and osteoblastic (*collagen type I alpha 1: Col1a1*; *osteocalcin: Ocn*; *receptor activator of NF- $\kappa$ B ligand: Rankl*; *osteoprotegerin: Opg*; *Wnt inhibitory factor 1: Wif1*; *Dickkopf-related protein 1: Dkk1*) marker mRNAs that responded to hypergravity and simulated g- $\mu$ G.

The isolation of total RNA and cDNA synthesis were performed using kits (Qiagen GmbH, Hilden, Germany) in accordance with the manufacturer's instructions (Suzuki et al., 2011; Ishizu et al., 2018). Each quantitative real time PCR reaction was performed using a real-time PCR apparatus (Mx3000p™, Stratagene, La Jolla, CA, USA). For the PCR reaction, a cDNA template mixed with the

appropriate primers was combined with SYBR Premix Ex Taq (Takara Bio Inc., Shiga, Japan) (Ikegame et al., 2019). The conditions for PCR amplification were 40 cycles of denaturation for 10 s at 95°C and annealing for 40 s at 60°C. The elongation factor 1 $\alpha$  (*Ef1 $\alpha$* ) was used for normalization. PCR primer sequences used in the current study are listed in Supplementary Table S1.

### Morphological analysis of osteoclasts in hypergravity- and simulated g- $\mu$ G-treated scales

#### *Hypergravity and simulated g- $\mu$ G treatment of the regenerating scales*

Sterilized regenerating scales were prepared as described above and then put into 96-well plates (one scale per well) with Leibovitz's L-15 medium (Invitrogen) containing 10% FCS (Nichirei Biosciences, Inc.), 100 U/mL of penicillin, 100  $\mu$ g/mL of streptomycin, and 200  $\mu$ g/mL of kanamycin. In the 3G loading, different parallel experiments using 10 goldfish were conducted. The 96-well plates containing the scales were loaded to 3G using a centrifuge (LIX-130, Tomy Digital Biology Co., Ltd., Tokyo, Japan) for 86 hours (Suzuki et al., 2008). This loading time is the same as the time of our space experiments (Ikegame et al., 2019). After centrifugation, the scales were fixed with 4% paraformaldehyde (PFA) in 0.1 M phosphate buffer (pH 7.4) for one night at 4°C. The fixed samples were transferred to PBS. The unloading was performed with a 3D clinostat (Toray Engineering Co., Ltd.). In the case of simulated g- $\mu$ G treatments, the regenerating scales were also prepared as described above and put into 96-well plates (one scale per well) and treated with a 3D clinostat for 86 hours. We performed the different parallel experiments using 10 goldfish as we did in hypergravity loading. After unloading with a 3D clinostat, the scales were fixed with 4% PFA in 0.1 M phosphate buffer (pH 7.4) for one night at 4°C. Then, the fixed samples were put into PBS.

#### *Actin staining*

The fixed specimens were incubated in 0.1% Triton X-100 for 10 min. F-actin was stained using 1% Alexa Fluor® 488 phalloidin (Molecular Probes, Eugene, OR, USA) in PBS for 4 days at 4°C in the dark. After rinsing in PBS, nuclear staining was performed using 4',6-diamidino-2-phenylindole (DAPI) (Dojindo Molecular Technologies, Inc., MD, USA), and then the specimens were observed under a fluorescence microscope (BX51; Olympus, Tokyo, Japan).

#### *TRAP staining*

The fixed specimens were stained for TRAP enzyme activity according to the modified method of Cole and Walters. Briefly, the scales were incubated in a solution containing naphthol AS-BI (0.1 mg/ml; Sigma–Aldrich) as a substrate, fast red violet (0.7 mg/ml; Sigma–Aldrich) as a diazonium-coupling salt, and 50 mM tartrate. Specimens were observed with a microscope (SZX10; Olympus).

#### *Histomorphometry*

Scales were randomly selected, and histomorphometric analysis was performed on six 0.31 mm<sup>2</sup> observation areas. Mean measurements from the six areas were regarded as representative values for each scale. The numbers of osteoclasts per mm<sup>2</sup> were recorded, and the mean number of nuclei per multinucleated osteoclast and the percentage of osteoclasts with actin rings were calculated. The width of the grooves at the middle of each groove, actin ring size, and the percentage of groove lengths covered with actin rings were measured using NIH Image J (<https://imagej.nih.gov/ij/>).

### Space experiment on the International Space Station

Goldfish were anesthetized, and their scales were removed one by one in two horizontal, bilateral lines using sharpened forceps. Subsequently, the goldfish were kept with a 12-h:12-h light–dark cycle (light turned on at 8:00 a.m.) at 26°C. On day 12 after removal of their scales, the goldfish were bred in water with the

anti-infection reagent F Gold (Japan Pet Design Co., Ltd., Tokyo, Japan). The next day, eight regenerating scales were collected from each goldfish ( $n = 40$ ) to measure the alkaline phosphatase (ALP) for osteoblast activity ( $n = 4$  regenerating scales) and TRAP for osteoclast activity ( $n = 4$  regenerating scales), and 14 individual goldfish with similar ALP and TRAP activities were selected from the 40 goldfish prepared, as described earlier. Subsequently, regenerating scales were sampled on day 14 from goldfish on ice that had been sterilized using hypochlorous and fungizone solutions and immersed in Leibovitz's L-15 medium (Invitrogen, Grand Island, NY, USA) containing 10% FCS (Nichirei Biosciences, Inc., Tokyo, Japan), 100 U/mL penicillin, 100  $\mu$ g/mL streptomycin, and 200  $\mu$ g/mL kanamycin. Sterilized goldfish scales were packed into Cell Exp Small Chamber culture chambers (Chiyoda Corp., Yokohama, Japan) (60 scales/chamber) and stored for 86 hours at 4°C before space shuttle STS-132 (ULF4) was launched to the International Space Station (ISS). The culture chambers were kept at 2.5°C–4.0°C and sent to the ISS via the Space Shuttle Atlantis (STS-132) (Yano, 2011) (see Supplementary Figure S2). After arrival on the ISS, they were incubated for 86 hours under microgravity at the Cell Biology Experiment Facility (CBEF) (Yano, 2011). The CBEF is equipped with a centrifuge to treat samples with one gravity [in-flight artificial microgravity (f-1G)] (Yano et al., 2012). This facility has the capability of culturing bio-specimens at a temperature range of 15–40°C (Yano et al., 2012). The differences among the sensors ranged from 0.1°C to 0.2°C (Yano et al., 2012). During incubation in the CBEF, culture chambers installed in the microgravity section (f- $\mu$ G) and 1G section (f-1G) of the CBEF were incubated at 21.9°C–22.0°C in the Measurement Experiment Unit (MEU) (Yano, 2011; Yano et al., 2012). The culture chambers were treated with 1G gravity in the 1G section, whereas they were kept without gravity treatment in the microgravity section. After incubation, the culture chambers were removed from the MEU. Then, the culture medium in the culture chamber was replaced with RNAlater (Sigma–Aldrich) for gene expression analysis. Japan Aerospace Exploration Agency astronaut Soichi Noguchi performed the above procedures exactly (see Supplementary Movie S1). Scales treated with RNAlater were stored at –96°C until the return of STS-132 to the Kennedy Space Center in Florida and analyzed for their biological characteristics.

### Global gene expression and pathway analyses

The deposited RNA-sequencing (RNA-seq) reads DRA008502 were re-analyzed to extract genes responsive to microgravity. The raw reads of RNA-seq were deposited at the DNA Data Bank of Japan (DDBJ; <https://ddbj.nig.ac.jp/DRASearch/submission?acc=DRA008502>) under the DDBJ Sequence Read Archive (DRA) accession no. DRA009188. Details regarding the library construction, sequencing, de novo transcriptome assembly, mapping, quantification, normalization, and annotation were previously described (Ikegame et al., 2019). Genes were considered differentially expressed genes (DEGs) where there was a log twofold change > 10.581 from the comparison between f-1G and f- $\mu$ G. The DEGs were further analyzed using Ingenuity® Pathway Analysis tools (Qiagen, Venlo, the Netherlands) (Tabuchi et al., 2006).

### Statistical analysis

All results are expressed as the means  $\pm$  SE. The statistical significance between the control and experimental groups was assessed by paired *t*-test. In all cases, the selected significance level was  $P < 0.05$ .

## RESULTS

### Influence of hypergravity (3G) by centrifuge on osteoclastic and osteoblastic marker mRNA expression

The effects of 3G loading on osteoclasts and osteo-



blasts are indicated in Figs. 1 and 2, respectively. By 3G loading, osteoclastic markers *Ctsk* and *Trap* mRNA expressions were significantly decreased. The mRNA expressions of *Oc-stamp*, *Itgb3*, and *c-Src* did not significantly change in the present conditions under 3G loading. On the other hand, osteoblastic markers *Ocn*, *Rankl*, and *Opg* mRNA expressions were significantly increased by 3G loading. The mRNA expression of *Dkk1* was significantly decreased by 3G loading. However, the levels of *Col1a1* and *Wif1* mRNA expression with 3G treatments did not differ from the control values.

#### Effects of simulated g- $\mu$ G with a 3D clinostat on osteoclastic and osteoblastic marker mRNA expression

The effects of simulated g- $\mu$ G on osteoclasts and osteoblasts are indicated in Figs. 3 and 4, respectively. All osteoclastic markers (*Ctsk*, *Trap*, *Oc-stamp*, *Itgb3*, and *c-Src*) investigated in the present study significantly increased. In osteoblasts, *Col1a1* mRNA expression was significantly suppressed under simulated g- $\mu$ G, while *Ocn* mRNA expression was not changed by simulated g- $\mu$ G loading. The mRNA expression of *Rankl* increased remarkably, although *Opg* mRNA expression was not changed by simu-

lated g- $\mu$ G treatments. *Wif1* and *Dkk1* mRNA expression levels increased significantly.

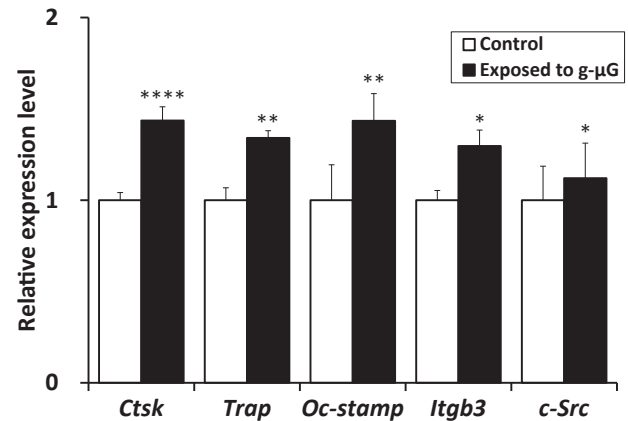


**Fig. 3.** Effects of simulated ground microgravity (g- $\mu$ G) on expression of osteoclastic marker genes. Values are mean  $\pm$  S.E.M. of 10 independent experiments. The value for the control sample was set as 1 for each gene. \*  $P < 0.05$  (Paired  $t$ -test), \*\*  $P < 0.01$  (Paired  $t$ -test), and \*\*\*\*  $P < 0.0001$  (Paired  $t$ -test).

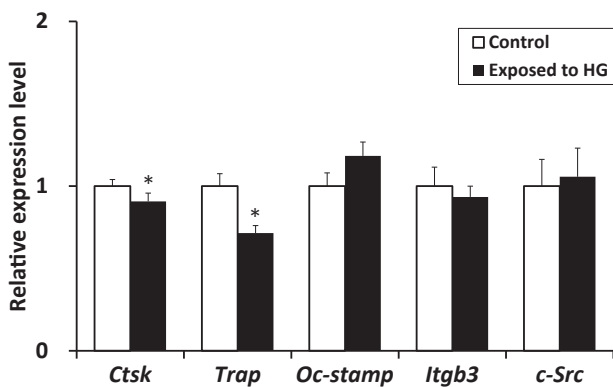


**Fig. 1.** Effects of hypergravity (HG) on expression of osteoclastic marker genes. Values are mean  $\pm$  S.E.M. of 10 independent experiments. The value for the control sample was set as 1 for each gene. \*  $P < 0.05$  (Paired  $t$ -test).

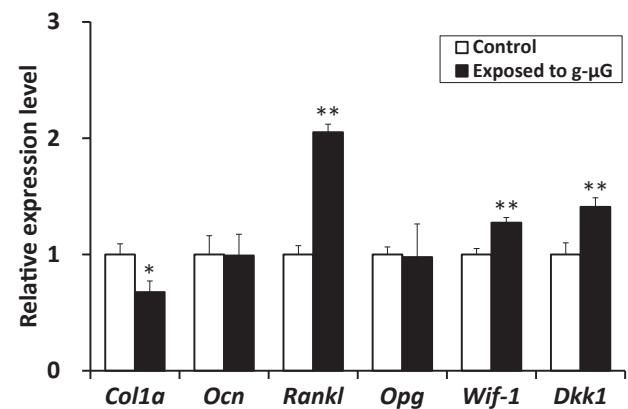


**Fig. 4.** Effects of simulated ground microgravity (g- $\mu$ G) on expression of osteoblastic marker genes. Values are mean  $\pm$  S.E.M. of 10 independent experiments. The value for the control sample was set as 1 for each gene. \*  $P < 0.05$  (Paired  $t$ -test) and \*\*  $P < 0.01$  (Paired  $t$ -test).

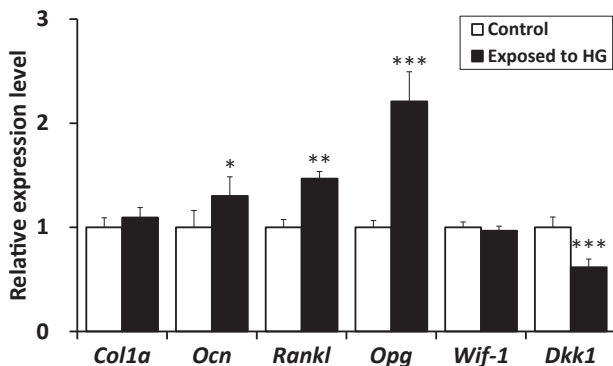


**Fig. 2.** Effects of hypergravity (HG) on expression of osteoblastic marker genes. Values are mean  $\pm$  S.E.M. of 10 independent experiments. The value for the control sample was set as 1 for each gene. \*  $P < 0.05$  (Paired  $t$ -test), \*\*  $P < 0.01$  (Paired  $t$ -test), and \*\*\*  $P < 0.001$  (Paired  $t$ -test).

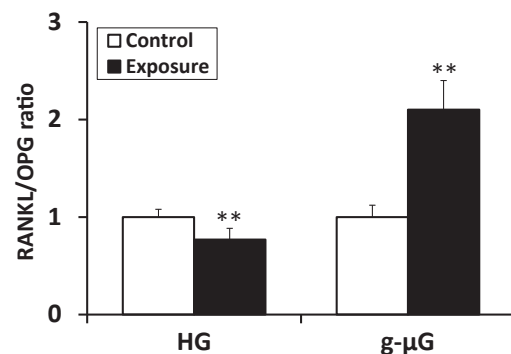


**Fig. 5.** The *Rankl*/*Opg* ratios under hypergravity (HG) and simulated ground microgravity (g- $\mu$ G). Values are mean  $\pm$  S.E.M. of 10 independent experiments. The value for the control sample was set as 1 for each gene. \*\*  $P < 0.01$  (Paired  $t$ -test).

### Changes in the *Rankl/Opg* ratio by hypergravity and simulated g- $\mu$ G

To examine the regulation of osteoclastic function, the ratio of *Rankl/Opg* was analyzed. The results are shown in Fig. 5. The *Rankl/Opg* ratio was significantly decreased by 3G loading. However, the ratio of *Rankl/Opg* was significantly increased by simulated g- $\mu$ G treatments.

### Morphological changes induced in osteoclasts by hypergravity and simulated g- $\mu$ G treatments

In osteoblasts, no significant change was induced by either hypergravity (3G) or simulated g- $\mu$ G treatments, at least under the present conditions. In the present study, we focused on osteoclasts and examined the morphological changes of osteoclasts in detail.

Osteoclasts having actin rings were mostly observed along the scale grooves (Fig. 6A–D). In these osteoclasts, we found that both the number of actin rings and the percentage of the lengths of grooves associated with the actin rings were significantly lower in the 3G-treated scales than in the control scales (Fig. 6E, F). However, the size of actin rings, the number of nuclei in multinucleated osteoclasts, and the number of osteoclast cells did not change significantly (Fig. 6G–I).

The results of simulated g- $\mu$ G treatments are shown in Fig. 7. The groove widths were significantly greater in the simulated g- $\mu$ G-treated scales than in the control scales (Fig. 7A–C).

The osteoclasts seemed larger, and the number of nuclei in multinucleated osteoclasts was significantly increased by simulated g- $\mu$ G treatments (Fig. 7F). This increase in the number of nuclei in multinucleated osteoclasts (Fig. 7F) was associated with a decrease of the number of mononucleated osteoclasts (Fig. 7D). In addition, the number of multinucleated osteoclasts exhibited no significant difference between the simulated g- $\mu$ G and control groups (Fig. 7E). The percentage of actin ring-positive multinucleated osteoclasts and the actin ring sizes were significantly

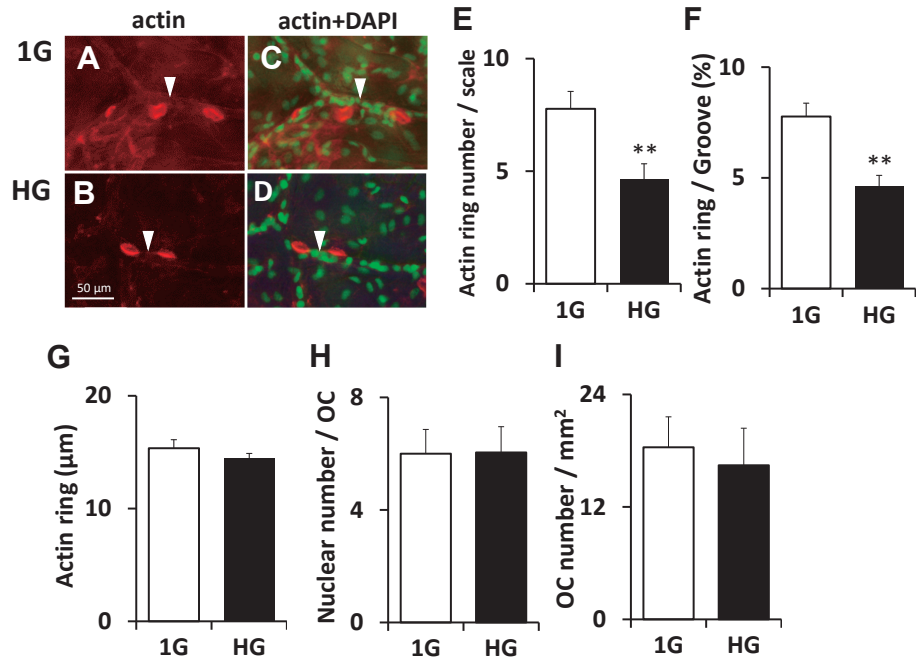


**Fig. 6.** Histomorphometric analysis of the osteoclasts treated with hypergravity (HG). (A–D) Fluorescence microscopy images of osteoclasts under control (1G) (A, C) or HG (3G) (B, D). F-actin staining (red) (A, B) superimposed on DAPI staining (green) of the nuclei (C, D). (E) The number of actin rings. (F) The percentage of the groove length covered by actin rings. (G) The average actin ring size measured as the diameter of the actin ring along the groove. (H) The average number of nuclei per multinucleated osteoclast. (I) The number of osteoclasts. Arrowheads indicate grooves in (A, B, C, D). Values are mean  $\pm$  S.E.M. of 10 independent experiments. \*\*  $P < 0.01$  (Paired  $t$ -test).

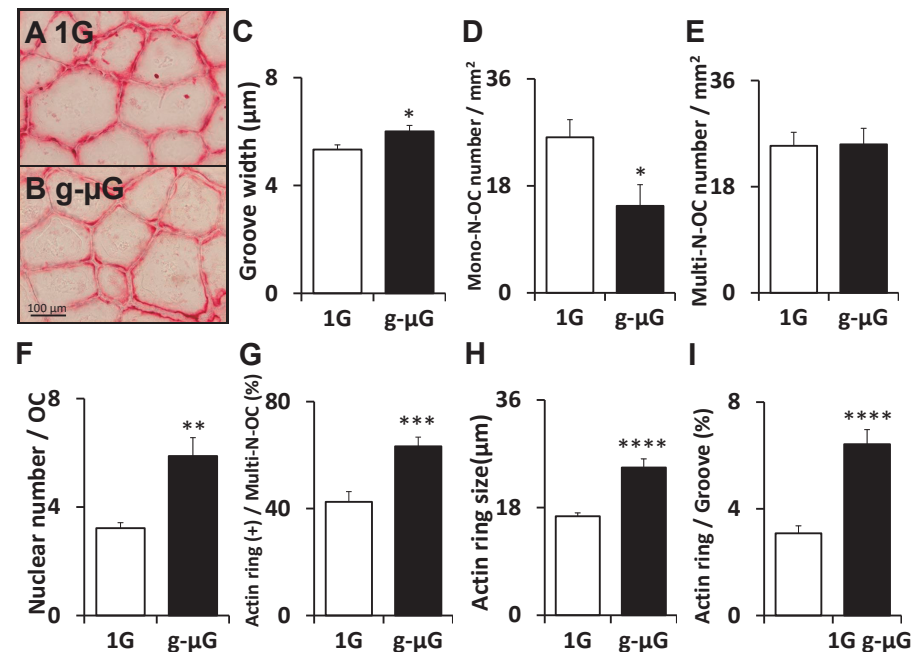


**Fig. 7.** Histomorphometric analysis of the osteoclasts treated with simulated ground-microgravity (g- $\mu$ G). (A, B) Light microscopy images of regenerating scales stained for TRAP activity under control (1G) (A) or simulated g- $\mu$ G (B). (C) Impact of simulated g- $\mu$ G on the groove width. (D) The average number of mononucleated osteoclasts. (E) The average number of multinucleated osteoclasts. (F) The average number of nuclei per multinucleated osteoclast. (G) The percentage of multinucleated osteoclasts with actin rings. (H) The average actin ring size measured as the diameter of the actin ring along the groove. (I) The percentage of the groove length covered by actin rings. Values are mean  $\pm$  S.E.M. of 10 independent experiments. \*  $P < 0.05$  (Paired  $t$ -test), \*\*  $P < 0.01$  (Paired  $t$ -test), \*\*\*  $P < 0.001$  (Paired  $t$ -test), and \*\*\*\*  $P < 0.0001$  (Paired  $t$ -test).

greater in the simulated g- $\mu$ G-treated scales (Fig. 7G, H) than in the control scales. Furthermore, since actin rings were mostly observed along scale grooves, the lengths of grooves associated with the actin rings were greater in simulated g- $\mu$ G-loaded scales than in the control scales (Fig. 7I).

### Changes in osteoclastic markers during space flight

During space flight, the mRNA expression of osteoclastic markers *Oc-stamp*, *Itgb3*, and *c-Src* increased (Fig. 8). Significant differences between f- $\mu$ G and f-1G were obtained in *Itgb3* mRNA expression.

### Global gene expression and pathway analyses during space flight

To identify the canonical pathways associated with space flight, the obtained data were analyzed with Ingenuity® Pathway Analysis tools. As a result, the Wnt/ $\beta$ -catenin pathway was predicted to be involved in the f- $\mu$ G response.

The data are shown in Fig. 9 and Supplementary Table S2. In particular, Fig. 9 depicts the canonical Wnt/ $\beta$ -catenin pathway, in which green-filled symbols indicate down-regulated genes under f- $\mu$ G. During space flight, several genes

involved in the canonical Wnt/ $\beta$ -catenin pathway were down-regulated. In particular, expressions of  $\beta$ -catenin-related genes were suppressed under f- $\mu$ G.

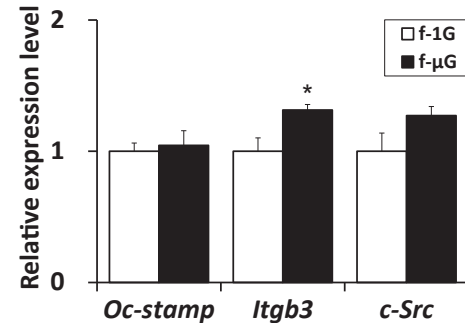


**Fig. 8.** Expression levels of osteoclastic marker genes under microgravity in outer space [Flight (f)- $\mu$ G] and under 1 G loading in outer space [Flight(f)-1G]. Values are mean  $\pm$  S.E.M. of four independent experiments. The value for the control sample was set as 1 for each gene. \*  $P < 0.05$  (Paired  $t$ -test).

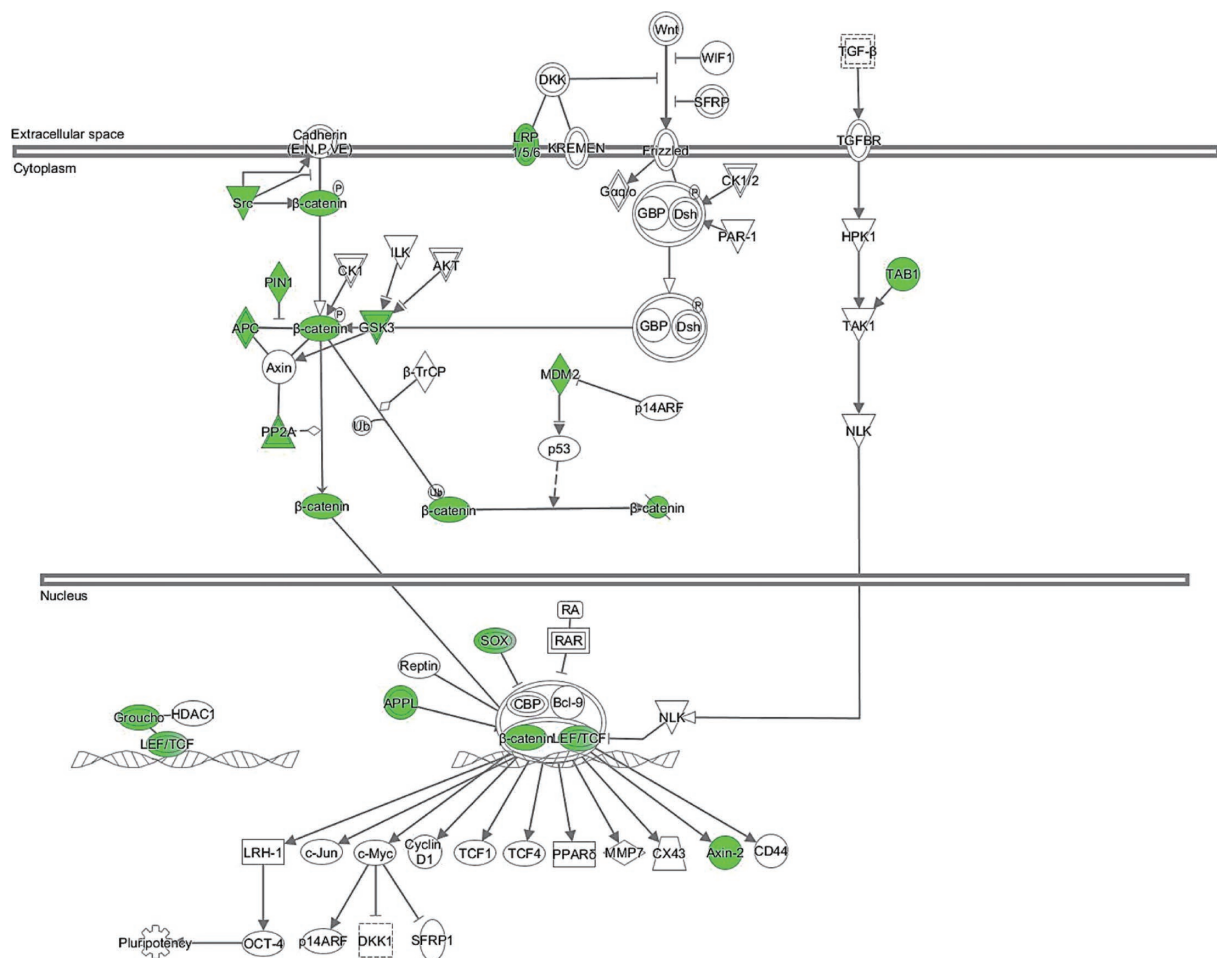


**Fig. 9.** Down-regulated genes linked to the canonical Wnt/ $\beta$ -catenin pathway during space flight. Genes that were differentially expressed in goldfish scales during space flight were analyzed using Ingenuity® Pathway Analysis tools. Expression levels of genes in the canonical Wnt/ $\beta$ -catenin pathway were down-regulated in goldfish scales cultured during space flight. Green-filled symbols indicate down-regulated genes.  $P$ -value:  $8.53 \times 10^{-4}$ .

## DISCUSSION

In the present study, we found that osteoclasts and osteoblasts in the scales of goldfish sensitively responded to hypergravity and simulated g- $\mu$ G when we analyzed these gravities using in vitro organ culture systems of osteoblasts and osteoclasts with intact bone matrix. To the best of our knowledge, this is the first study that has examined the respective responses of both osteoclasts and osteoblasts to hypergravity and simulated g- $\mu$ G at the same time. Namely, we found that 3G loading altered the mRNA expression of both osteoclastic and osteoblastic markers and functioned to induce bone formation (Fig. 1, 2). Under simulated g- $\mu$ G, on the other hand, the mRNA expression of osteoclastic markers increased remarkably (Fig. 3), but osteoblastic marker mRNA expression decreased (Fig. 4). These markers functioned to induce bone resorption under simulated g- $\mu$ G. Furthermore, judging from morphological observations, osteoclastic deactivation was induced by 3G loading (Fig. 6), while osteoclastic activation was promoted under simulated g- $\mu$ G (Fig. 7). These changes induced in osteoclasts and osteoblasts of goldfish scales by hypergravity and simulated g- $\mu$ G were consistent with mammalian in vivo studies (Kawao et al., 2016; Chatziravdeli et al., 2019; Smith, 2020). These results strongly suggest that our in vitro organ culture system is an excellent model for analyzing bone metabolism in gravity.

Several studies of hypergravity with mammalian osteoblastic cells have been reported. Osteoblastic responses have been investigated by applying high-G loading from 5 to 50 G, and osteoblastic activation by high-G loading was reported (Gebken et al., 1999; Saito et al., 2003; Searby et al., 2005; Zhou et al., 2015). Scale osteoblasts as well as mammalian osteoblasts (Gebken et al., 1999; Saito et al., 2003; Searby et al., 2005; Zhou et al., 2015) sensitively responded and were activated by low-G (3G) loading (Fig. 2). In the case of mammalian osteoclasts, hypergravity did not cause a clear response (Nemoto and Uemura, 2000). In short, isolated osteoclasts from rabbits were cultured on ivory and exposed to 30 G for 2 hr or 18 hr by placing the culture tubes in a swinging bucket rotor. As a result, there was no hypergravity effect on the numbers of activated osteoclasts with actin ring formation (Nemoto and Uemura, 2000). It is necessary to consider various conditions of gravity loading with mammalian osteoclasts. Interestingly, in an in vivo study with mice, 3G loading by centrifugation significantly increased trabecular bone mineral content and induced bone formation (Kawao et al., 2016). That in vivo study indicated that osteoblasts and osteoclasts respond without the application of high gravity. Thus, our organ culture system with fish scales can analyze bone metabolism in a state close to in vivo, because 3G hypergravity loading induced responses in osteoclasts and osteoblasts of the scales, as did 3G hypergravity in mammalian in vivo studies. Additionally, in the reported studies of cell culture with mammalian osteoclasts and osteoblasts under simulated g- $\mu$ G, osteoclastic responses did not agree with those of the in vivo studies during space flight (Makihara et al., 2008; Chatziravdeli et al., 2019; Smith, 2020). It has been reported that osteoclast activation did not occur, resulting from the suppression of *Rankl* mRNA expression under simulated g- $\mu$ G (Makihara et al., 2008). Interestingly, our ground basis

results by simulated g- $\mu$ G were mostly consistent with those of our space experiment (Ikegame et al., 2019; Smith, 2020). Taking these results into consideration together with our obtained results, the results obtained with our fish scale organ culture are quite similar to those of mammalian in vivo studies and our fish scale organ culture has a good response to both hypergravity and microgravity.

It is known that osteoclasts are regulated by interaction with osteoblasts (Kondo et al., 2001; Kearns et al., 2008; Lacey et al., 2012). Namely, the fusion of pre-osteoclasts to become multinucleated osteoclasts (active type of osteoclasts) is induced by binding RANKL in an osteoblast to the receptor activator of nuclear factor- $\kappa$ B (RANK) in an osteoclast. In addition, osteoprotegerin (OPG), which is produced by osteoblasts, is a decoy receptor of RANKL and suppresses osteoclastogenesis (Kubota et al., 2009; Silva and Branco, 2011; Lacey et al., 2012). As described above, osteoclastic activation is regulated by RANK/RANKL and OPG. In the present study, therefore, we analyzed expression of genes encoding these molecules. 3G hypergravity significantly decreased the ratio of *Rankl*/*Opg*, while simulated g- $\mu$ G increased the ratio of *Rankl*/*Opg* (Fig. 5). Therefore, this difference is dependent on the fact that the hypergravity increased *Opg* expression (Fig. 2) while the simulated g- $\mu$ G did not (Fig. 4). Accordingly, inhibitors (WIF1 and DKK1) of the Wnt/ $\beta$ -catenin signaling pathway, an important signaling pathway regulating OPG expression (Kubota et al., 2009; Silva and Branco, 2011) were then analyzed in the present study. By 3G loading, *Dkk1* mRNA expression was significantly decreased (Fig. 2), while the expression of *Dkk1* mRNA was significantly increased under simulated g- $\mu$ G (Fig. 4). *Wif1* mRNA expression increased significantly under simulated g- $\mu$ G (Fig. 4), while it did not change under the condition of 3G hypergravity (Fig. 2).

We found that both hypergravity and simulated g- $\mu$ G increased the expression of *Rankl*. This result indicates that the *Rankl* gene may be sensitive to altered gravity in general. In accord with this idea, a previous study using human cells searched for genes that are differentially expressed in both microgravity and hypergravity and revealed that both microgravity and hypergravity suppress the expression of the G-protein coupled receptor OR12D3, as well as the levels of three non-coding RNAs (RNUD-1, SNORD63, and AC083843.1) (Thiel et al., 2017).

To confirm the results obtained by simulated g- $\mu$ G treatments, we performed space experiments and examined the influence of f- $\mu$ G on bone metabolism. During space flight, we found that the mRNA expression of osteoclastic markers *Oc-stamp*, *Itgb3*, and *c-Src* increased. It has been reported that gravitational changes alter expression levels of various genes and that interaction among the changes in gene expression plays a critical role in the cellular response to gravitational changes (Cavanagh et al., 2005; Smith, 2020). Therefore, we comprehensively examined the effects of microgravity in outer space on gene expression in the fish scale model of the bone. As a result, we found that the Wnt/ $\beta$ -catenin pathway was involved in the responses of bone cells in the fish scale model of the bone to f- $\mu$ G. Notably, the Wnt/ $\beta$ -catenin pathway was found to play an important role in the responses of bone cells to gravitational changes (Lin et al., 2009). During space flight, several genes involved in



the Wnt/ $\beta$ -catenin pathway were down-regulated. These results agreed with the results of simulated g- $\mu$ G (Figs. 3–5).

Since osteoblasts and osteoclasts are distributed on their surface, fish scales have the excellent feature that morphological analysis with the whole mount can be facilitated (Kobayashi et al., 2016; Suzuki et al., 2016; Ikegame et al., 2019). By simulated g- $\mu$ G treatments, the size of osteoclasts was increased, and the number of nuclei in multinucleated osteoclasts was significantly greater as compared with that of 1G control scales (Fig. 7). Most of the activated osteoclasts were distributed along the edges of the grooves in the scales (Fig. 7). Quite interestingly, we reported that RANKL-producing cells were present in the grooves of regenerating scales and were distributed in contact with multinucleated osteoclasts (Yamamoto et al., 2020b). This strongly suggests that osteoclasts activated by RANKL secreted from the RANKL-producing cells existed in the groove. Under simulated g- $\mu$ G treatments, the increase of mRNA expression of *Oc-stamp* that is associated with multinucleation in osteoclasts (Fig. 3; Yamamoto et al., 2020b) was supported by the above results. Until now, there have been several reports regarding osteoclastic activation under microgravity, including simulated g- $\mu$ G (Rucci et al., 2007; Tamma et al., 2008; Smith, 2020). However, no studies have investigated osteoclastic morphological changes in detail under hypergravity. We are the first to demonstrate hypergravity and g- $\mu$ G responses to osteoclasts morphologically using the same methods.

In addition to responses to gravitational changes, we previously reported that the stimuli of low-intensity pulsed ultrasound (LIPUS) can be detected by osteoblasts in goldfish scales and promote the regeneration of goldfish scales (Hanmoto et al., 2017). In the scales of zebrafish, LIPUS was found to increase expression of osteoblastic genes and was reported to induce apoptosis of osteoclasts (Suzuki et al., 2016). Furthermore, a previous study found that activities of both osteoclasts and osteoblasts in the scales of medaka are altered in response to hypergravity (Yano et al., 2013). The findings of the current study, together with the above-mentioned findings using fish scales, provide evidence that the organ culture systems of fish scales, in which osteoclasts and osteoblasts coexist on the intact bone matrix and respond sensitively to gravitational changes, are an excellent experimental system for studying responses of bone cells to gravity changes during space flight.

## ACKNOWLEDGMENTS

This study was supported in part by grants to NS (Grant-in-Aid for Scientific Research [C] No. 20K06718 by JSPS), to AH (Grant-in-Aid for Scientific Research [C] No. 18K11016 by JSPS), to YT (Grant-in-Aid for Scientific Research [C] No. 20K12619 by JSPS), and to JH (Grant-in-Aid for Scientific Research [B] No. 20H04565 and [C] No. 18KT0068 by JSPS). This work was partly supported by the cooperative research program of the Institute of Nature and Environmental Technology, Kanazawa University, Accept Nos. 21021, 21023, 21024, and 21046.

## COMPETING INTERESTS

The authors declare that they have no conflict of interest.

## AUTHOR CONTRIBUTIONS

Experimental design: NS, AH, TS, and HM. Conduct of experiments: TY, MI, YF, YT, UK, JH, SY, KK, ME, AN, YM, KW, and KH.

Interpretation of data: TY, NS, AH, YF, and YT. Writing of the manuscript: NS, TY, AH, YF, YT and JH.

## SUPPLEMENTARY MATERIALS

Supplementary materials for this article are available online. (URL: <https://doi.org/10.2108/zs210107>)

**Supplementary Figure S1.** Photograph of three-dimensional clinostat.

**Supplementary Figure S2.** Space shuttle STS-132 launched to the International Space Station (ISS).

**Supplementary Table S1.** Sequences of primers used for quantitative real-time PCR analysis.

**Supplementary Table S2.** List of down-regulated genes.

**Supplementary Movie S1.** An astronaut processes biological samples under microgravity on the ISS. JAXA astronaut Soichi Noguchi manipulates a Pre-Fixation Kit to exchange the culture medium from culture chambers inside the kit. Each time he grabs and releases the handle of the Pre-Fixation Kit, the syringes inside the kit push the medium from the chamber into the waste medium bag set behind the kit. During the operation, he checks to see if the medium is collecting in the waste bag.

## REFERENCES

- Alford AI, Kozloff KM, Hankenson KD (2015) Extracellular matrix networks in bone remodeling. *Int J Biochem Cell Biol* 65: 20–31
- Bereiter-Hahn J, Zylberberg L (1993) Regeneration of teleost fish scale. *Comp Biochem Physiol* 105A: 625–641
- Carmeliet G, Vico L, Bouillon R (2001) Space flight: A challenge for normal bone homeostasis. *Crit Rev Eukaryot Gene Expr* 11: 131–144
- Cavanagh PR, Licata AA, Rice AJ (2005) Exercise and pharmacological countermeasures for bone loss during long-duration space flight. *Gravit Space Biol Bull* 18: 39–58
- Chatziravdeli V, Katsaras GN, Lambrou GI (2019) Gene expression in osteoblasts and osteoclasts under microgravity conditions: A systematic review. *Curr Genomics* 20: 184–198
- Chen X, Wang Z, Duan N, Zhu G, Schwarz EM, Xie C (2018) Osteoblast–osteoclast interactions. *Connect Tissue Res* 59: 99–107
- Civitelli R (2008) Cell–cell communication in the osteoblast/osteocyte lineage. *Arch Biochem Biophys* 473: 188–192
- Gebken J, Lüders B, Notbohm H, Klein HH, Brinckmann J, Müller PK, et al. (1999) Hypergravity stimulates collagen synthesis in human osteoblast-like cells: Evidence for the involvement of p44/42 MAP-kinases (ERK 1/2). *J Biochem* 126: 676–682
- Hanmoto T, Tabuchi Y, Ikegame M, Kondo T, Kitamura K, Endo M, et al. (2017) Effects of low-intensity pulsed ultrasound on osteoclasts: Analysis with goldfish scales as a model of bone. *Biomed Res* 38: 71–77
- Harter LV, Hruska KA, Duncan RL (1995) Human osteoblast-like cells respond to mechanical strain with increased bone matrix protein production independent of hormonal regulation. *Endocrinology* 136: 528–535
- Hoffler CE, Hankenson KD, Miller JD, Bilkhu SK, Goldstein SA (2006) Novel explant model to study mechanotransduction and cell–cell communication. *J Orthop Res* 24: 1687–1698
- Ikegame M, Hattori A, Tabata MJ, Kitamura K, Tabuchi Y, Furusawa Y, et al. (2019) Melatonin is a potential drug for the prevention of bone loss during space flight. *J Pineal Res* 67: e12594
- Ishizu H, Sekiguchi T, Ikari T, Kitamura KI, Kitani Y, Endo M, et al. (2018)  $\alpha$ -Melanocyte-stimulating hormone promotes bone resorption resulting from increased osteoblastic and osteoclastic activities in goldfish. *Gen Comp Endocrinol* 262: 99–105
- Kawao N, Morita H, Obata K, Tamura Y, Okumoto K, Kaji H (2016) The vestibular system is critical for the changes in muscle and bone induced by hypergravity in mice. *Physiol Rep* 4: e12979
- Kearns AE, Khosla S, Kostenuik PJ (2008) Receptor activator of

- nuclear factor kappaB ligand and osteoprotegerin regulation of bone remodeling in health and disease. *Endocr Rev* 29: 155–192
- Kobayashi Y, Uehara S, Udagawa N, Takahashi N (2016) Regulation of bone metabolism by Wnt signals. *J Biochem* 159: 387–392
- Kondo Y, Irie K, Ikegame M, Ejiri S, Hanada K, Ozawa H (2001) Role of stromal cells in osteoclast differentiation in bone marrow. *J Bone Miner Metab* 19: 352–358
- Kubota T, Michigami T, Ozono K (2009) Wnt signaling in bone metabolism. *J Bone Miner Metab* 27: 265–271
- Lacey DL, Boyle WJ, Simonet WS, Kostenuik PJ, Dougall WC, Sullivan JK, et al. (2012) Bench to bedside: Elucidation of the OPG-RANK-RANKL pathway and the development of denosumab. *Nat Rev Drug Discov* 11: 401–419
- Lin C, Jiang X, Dai Z, Guo X, Weng T, Wang J, et al. (2009) Sclerostin mediates bone response to mechanical unloading through antagonizing Wnt/ $\beta$ -catenin signaling. *J Bone Miner Res* 24: 1651–1661
- Makihira S, Kawahara Y, Yuge L, Mine Y, Nikawa H (2008) Impact of the microgravity environment in a 3-dimensional clinostat on osteoblast- and osteoclast-like cells. *Cell Biol Int* 32: 1176–1181
- Nemoto A, Uemura T (2000) Hypergravity effects on osteoclasts activity. *J Gravit Physiol* 7: 127–128
- Nishimoto SK, Araki N, Robinson FD, Waite JH (1992) Discovery of bone  $\gamma$ -carboxyglutamic acid protein in mineralized scales. *J Biol Chem* 267: 11600–11605
- Ohira Y, Shimizu M, Ura K, Takagi Y (2007) Scale regeneration and calcification in goldfish *Carassius auratus*: Quantitative and morphological processes. *Fisheries Sci* 73: 46–54
- Omori K, Wada S, Maruyama Y, Hattori A, Kitamura K, Sato Y, et al. (2012) Prostaglandin  $E_2$  increases both osteoblastic and osteoclastic activities in the scales and participates in the calcium metabolism in goldfish. *Zool Sci* 29: 499–504
- Onozato H, Watabe N (1979) Studies on fish scale formation and resorption III: Fine structure and calcification of the fibrillary plates of the scales in *Carassius auratus* (Cypriniformes: Cyprinidae). *Cell Tissue Res* 201: 409–422
- Owan I, Burr DB, Turner CH, Qiu J, Tu Y, Onyia JE, et al. (1997) Mechanotransduction in bone: Osteoblasts are more responsive to fluid forces than mechanical strain. *Am J Physiol* 273: C810–C815
- Rucci N, Rufo A, Alamanou M, Teti A (2007) Modeled microgravity stimulates osteoclastogenesis and bone resorption by increasing osteoblast RANKL/OPG ratio. *J Cell Biochem* 100: 464–473
- Saito M, Soshi S, Fujii K (2003) Effect of hyper- and microgravity on collagen post-translational controls of MC3T3-E1 osteoblasts. *J Bone Miner Res* 18: 1695–1705
- Schaffler MB, Kennedy OD (2012) Osteocyte signaling in bone. *Curr Osteoporosis Rep* 10: 118–125
- Searby ND, Steele CR, Globus RK (2005) Influence of increased mechanical loading by hypergravity on the microtubule cytoskeleton and prostaglandin  $E_2$  release in primary osteoblasts. *Am J Physiol* 289: C148–C158
- Silva I, Branco JC (2011) RANK/RANKL/OPG: Literature review. *Acta Reumatol Port* 36: 209–218
- Smith JK (2020) Osteoclasts and microgravity. *Life* 10: 207
- Suzuki N, Hattori A (2002) Melatonin suppresses osteoclastic and osteoblastic activities in the scales of goldfish. *J Pineal Res* 33: 253–258
- Suzuki N, Suzuki T, Kurokawa T (2000) Suppression of osteoclastic activities by calcitonin in the scales of goldfish (freshwater teleost) and nibbler fish (seawater teleost). *Peptides* 21: 115–124
- Suzuki N, Kitamura K, Nemoto T, Shimizu N, Wada S, Kondo T, et al. (2007) Effect of vibration on osteoblastic and osteoclastic activities: Analysis of bone metabolism using goldfish scale as a model for bone. *Adv Space Res* 40: 1711–1721
- Suzuki N, Omori K, Nakamura M, Tabata MJ, Ikegame M, Ijiri K, et al. (2008) Scale osteoblasts and osteoclasts sensitively respond to low-gravity loading by centrifuge. *Biol Sci Space* 22: 3–7
- Suzuki N, Kitamura K, Omori K, Nemoto T, Satoh Y, Tabata MJ, et al. (2009) Response of osteoblasts and osteoclasts in regenerating scales to gravity loading. *Biol Sci Space* 23: 211–217
- Suzuki N, Danks JA, Maruyama Y, Ikegame M, Sasayama Y, Hattori A, et al. (2011) Parathyroid hormone 1 (1-34) acts on the scales and involves calcium metabolism in goldfish. *Bone* 48: 1186–1193
- Suzuki N, Hanmoto T, Yano S, Furusawa Y, Ikegame M, Tabuchi Y, et al. (2016) Low-intensity pulsed ultrasound induces apoptosis in osteoclasts: Fish scales are a suitable model for analysis of bone metabolism by ultrasound. *Comp Biochem Physiol Part A* 195: 26–31
- Tabuchi Y, Takasaki I, Doi T, Ishii Y, Sakai H, Kondo T (2006) Genetic networks responsive to sodium butyrate in colonic epithelial cells. *FEBS Lett* 580: 3035–3041
- Tamma R, Colaianni G, Camerino C, Di Benedetto A, Greco G, Strippoli M, et al. (2008) Microgravity during spaceflight directly affects in vitro osteoclastogenesis and bone resorption. *FASEB J* 23: 2549–2554
- Tatsumi S, Ishii K, Amizuka N, Li M, Kobayashi T, Kohno K, et al. (2007) Targeted ablation of osteocytes induces osteoporosis with defective mechanotransduction. *Cell Metab* 5: 464–475
- Thamamongkood TA, Furuya R, Fukuba S, Nakamura M, Suzuki N, Hattori A (2012) Expression of osteoblastic and osteoclastic genes during spontaneous regeneration and autotransplantation of goldfish scale: A new tool to study intramembranous bone regeneration. *Bone* 50: 1240–1249
- Thiel CS, Hauschild S, Hugel A, Tauber S, Lauber BA, Polzer J, et al. (2017) Dynamic gene expression response to altered gravity in human T cells. *Sci Rep* 7: 5204
- Watabe H, Furuhama T, Tani-Ishii N, Mikuni-Takagaki Y (2011) Mechanotransduction activates  $\alpha_5\beta_1$  integrin and PI3K/Akt signaling pathways in mandibular osteoblasts. *Exp Cell Res* 317: 2642–2649
- Yamamoto T, Ikegame M, Hirayama J, Kitamura K, Tabuchi Y, Furusawa Y, et al. (2020a) Expression of sclerostin in the regenerating scales of goldfish and its increase under microgravity during space flight. *Biomed Res (Tokyo)* 41: 279–288
- Yamamoto T, Ikegame M, Kawago U, Tabuchi Y, Hirayama J, Sekiguchi T, et al. (2020b) Detection of RANKL-producing cells and osteoclastic activation by the addition of exogenous RANKL in the regenerating scales of goldfish. *Biol Sci Space* 34: 34–40
- Yano S (2011) Preparation and overview of fish scales experiment. *Space Utiliz Res* 27: 213–216
- Yano S, Masuda D, Kasahara H, Omori K, Higashibata A, Asashima M, et al. (2012) Excellent thermal control ability of cell biology experiment facility (CBEF) for ground-based experiments and experiments onboard the Kibo Japanese experiment module of international space station. *Biol Sci Space* 26: 12–20
- Yano S, Kitamura K, Satoh Y, Nakano M, Hattori A, Sekiguchi T, et al. (2013) Static and dynamic hypergravity responses of osteoblasts and osteoclasts in medaka scales. *Zool Sci* 30: 217–223
- Yoshikubo H, Suzuki N, Takemura K, Hosono M, Yashima S, Iwamuro S, et al. (2005) Osteoblastic activity and estrogenic response in the regenerating scale of goldfish, a good model of osteogenesis. *Life Sci* 76: 2699–2709
- Zhou S, Zu Y, Sun Z, Zhuang F, Yang C (2015) Effects of hypergravity on osteopontin expression in osteoblasts. *PLOS ONE* 10: e0128846
- Zylberberg L, Bonaventure J, Cohen-Solal L, Hartmann DJ, Bereiter-Hahn J (1992) Organization and characterization of fibrillar collagens in fish scales in situ and in vitro. *J Cell Sci* 103: 273–285

(Received November 23, 2021 / Accepted February 13, 2022 / Published online April 5, 2022)